The Astronomical Journal, 124:1118–1126, 2002 August

WIDE BINARY SYSTEMS AND THE NATURE OF HIGH-VELOCITY WHITE DWARFS[1]

Nicole M. Silvestri and Terry D. Oswalt
Department of Physics and Space Sciences and the SARA Observatory, Florida Institute of Technology,
150 West University Boulvard, Melbourne, FL 32901-6975; nicole@astro.fit.edu, oswalt@astro.fit.edu

and

Suzanne L. Hawley
Department of Astronomy, University of Washington, Seattle, WA 98195;
slh@pillan.astro.washington.edu
Received 2002 March 13; accepted 2002 April 22

ABSTRACT

We present measured radial velocities and complete space motions for 116 white dwarf stars with M dwarf companions. Thirteen pairs have "halo-like" velocities. According to a recent study by Oppenheimer et al., all these high-velocity white dwarfs should be considered part of the dark matter heavy halo of the Galaxy, based on their kinematics. Based on the near-solar abundance levels of the M dwarf companions, we conclude that 12 of our 13 high-velocity white dwarfs are actually part of the high-velocity tail of the thick disk, rather than the dark matter halo of the Galaxy, in agreement with the results of a recent study of 514 M dwarfs performed by Reid, Sahu, & Hawley. We find only one potential stellar halo white dwarf (LP 164-52) in our sample. The M dwarf companion of LP 164-52 is a metal-poor, intermediate subdwarf with high-velocity *UVW*-space motions. In view of the similarity to our sample, we conclude that the majority of the dark matter halo white dwarfs identified by Oppenheimer et al. are most likely to be members of the thick disk, and hence their contribution to the dark matter content of the halo is very much overestimated. Our results suggest that the assignment of population membership solely on incomplete kinematical information is not definitive and that a more robust examination of suspected halo white dwarfs must be performed.

Key words: binaries: general — Galaxy: disk — Galaxy: kinematics and dynamics — stars: fundamental parameters — white dwarfs

1. INTRODUCTION

Dark matter has been attributed to many different sources over the years, from exotic particles to brown dwarfs (see Reid, Sahu, & Hawley 2001, hereafter RSH, and references therein). White dwarf (WD) stars, the remnants of stars with masses less than 8 $M_\odot$, have recently become the center of attention in the controversy over the dark matter content of the Galaxy's heavy halo. The recent mass limits placed on the objects responsible for the majority of microlensing events observed by the MACHO project ($\langle M \rangle = 0.5 \pm 0.3\ M_\odot$; Alcock et al. 2000) are suspiciously similar to WDs whose typical masses are $0.5\ M_\odot < M_{\rm WD} < 0.7\ M_\odot$ (see, for example, Reid 1996; Silvestri et al. 2001, and references therein).

The recent realization that the photometric colors of cool WDs are profoundly affected by the onset of H_2 molecular opacity for $T_{\rm eff} \leq 4500$ K has also sparked new interest in this subset of WDs. Such objects are often dubbed ultracool WDs or cool blue degenerates (CBDs). As demonstrated by Bergeron et al. (1994), Hansen (1998), and Saumon & Jacobson (1999), the collisionally induced H_2 molecular opacity in CBD atmospheres results in heavy blanketing in the red to infrared portion of the spectrum. Such objects appear bluer in color than a blackbody spectrum would exhibit at the WD's temperature. Thus the oldest, coolest WDs are bluer than candidates targeted by previous surveys. This raises the possibility that CBDs may be part of a previously overlooked dark matter halo population of WDs (see, for example, Ibata et al. 2000; Bergeron 2001).

Recent surveys have yielded several dozen new stellar halo WD candidates (Hambly et al. 1999; Knox, Hawkins, & Hambly 1999; Mendez & Minniti 2000; Oppenheimer et al. 2001b). Oppenheimer et al. (2001a, hereafter OHDHS) identified an unprecedented number of potential dark matter halo candidates in a sample of 99 high–proper-motion WDs. In a field of over 4100 deg^2 of sky near the south Galactic polar cap, OHDHS used reduced proper motion diagrams restricted to objects with proper motions ($\mu \geq 0\farcs33$ yr^{-1}) to isolate halo WD candidates. Specifically, OHDHS used estimates of the *UV*-space motions to separate presumed halo WDs in their sample from WDs in the disk of the Galaxy. Because radial velocities, hence full space motions, cannot be determined for single WDs, OHDHS chose to assume that near the south Galactic cap $W = 0$ km s^{-1}. They argued that because the two populations (halo and disk) have different tangential velocities (v_t) such partial space motions can be used to determine population membership. From the objects selected for spectroscopic observation, OHDHS found 38 WDs in their survey with "halo-like" (high) velocities. From an analysis of these data OHDHS derived a dark matter halo mass density of $1.3 \times 10^{-4}\ M_\odot$ pc^{-3}. This value is roughly an order of magnitude larger than expected (Gould, Flynn, & Bahcall 1998).

[1] Based on observations obtained with the Apache Point Observatory 3.5 m telescope, which is owned and operated by the Astrophysical Research Consortium, and the SARA Observatory at Kitt Peak, which is owned and operated by the Southeastern Association for Research in Astronomy.

For obvious reasons the OHDHS study has sparked a lively response. Most of the discussion has centered on the kinematics of the OHDHS WDs and their resultant population membership: thin disk, thick disk, stellar halo, and dark matter halo (for a detailed discussion of the differences between the stellar and dark matter halo refer to RSH and references therein). Gibson & Flynn (2002) argued that the OHDHS sample is far less complete than claimed, resulting in a significantly smaller mass density than the one OHDHS derived. Koopmans & Blandford (2002) analyzed the kinematics of the OHDHS sample and determined that the sample's space motions are most consistent with a two-component population in which the majority of WDs are from the thick disk, with at most a few percent from the stellar halo. Davies, King, & Ritter (2002) computed a plausible scenario in which all the OHDHS high-velocity WDs could have originated in the Galactic disk as main-sequence components of close binaries that were disrupted during Type II supernova events. Using a complete sample of 514 M dwarf (dM) stars RSH showed that the majority of the high-velocity WDs in the OHDHS study have *UV*-velocities similar to the 20 high-velocity dM's in their sample. RSH pointed out that the metallicities of the 20 high-velocity dM's belong to the high-velocity tail of the thick disk (see their Figs. 3 and 4). The percentage of stars in OHDHS with retrograde motions implies a number density representative of the stellar halo and suggests that *none* of the 38 high-velocity WDs in the OHDHS sample need be members of the dark matter halo. Hansen (2001), using new cool WD atmosphere models, determined that the age distribution of the OHDHS WDs agrees best with the standard thin-disk WD population. Very recently, Reylé, Robin, & Crézé (2001), based on their simulations of Galactic stellar populations, concluded that the OHDHS WDs are part of the thick disk. Thus, it is unclear whether OHDHS have really measured an observable component of the dark matter halo or whether the WD population they have identified can be accommodated in a conventional model of visible Galactic populations (thin disk, thick disk, and stellar halo).

Here we describe the results of a study of WDs in wide binaries that have comparable space motions to the OHDHS WDs. These WDs have dM companions (WD + dM). Unlike studies of single WDs, our pairs permit the determination of full space motions of the WDs from the radial velocities (v_r) of their dM companions (Silvestri et al. 2001). As demonstrated by RSH, the metallicity of the dM's firmly constrains the population membership of the WDs because the disk and halo populations are chemically distinct from one another (Gizis 1997). If it can be shown that a substantial sample of WDs like ours with space motions similar to the OHDHS sample have companions with metallicities that constrain them to the Galactic disk population, this would likewise constrain the population membership of the OHDHS WDs. We address this idea in the following sections.

In § 2 we present an overview of the observations and reductions for our sample. A discussion of the kinematics and sample differences with respect to the OHDHS sample is given in § 3. The interpretation of the kinematic results and comparison with known Galactic populations is presented in § 4. We conclude with a discussion of the results and implications of our findings in § 5.

2. OBSERVATIONS AND DATA

As outlined in § 1, the existence of a dM companion provides a unique way of determining population membership for a WD. The wide binaries used in this study are a subset of a large proper motion–selected sample of ~500 pairs with suspected WD components originally found by Luyten (1963, 1969, 1974, 1979) and Giclas, Burnham, & Thomas (1971, 1978). Low-resolution spectra (7–15 Å pixel^{-1}; Oswalt, Hintzen, & Luyten 1988; Oswalt et al. 1991, 1993) confirmed nearly 300 new WDs in this sample. *BVRI* photometry of most of these pairs was obtained by Smith (1997).

For the present study we selected a subset of over 100 binaries, which proved to contain WD + dM components. The sole selection criterion for inclusion in this study was that each system must contain a spectroscopically identified WD and a dM star. The biases in our sample imposed by sampling area, proper motion (μ), and limiting apparent magnitude (photographic magnitude m_{pg}) of the original surveys are well understood (see Oswalt & Smith 1995; Smith & Oswalt 1995; Oswalt et al. 1996; Wood & Oswalt 1998). The Luyten proper-motion survey, from which most of our objects are drawn, includes objects from the entire sky north of declination -33° except for the most dense regions of the Galactic plane ($|b| < 15^\circ$), covering ~65% of the visible sky (Dawson 1986). The binaries are restricted to $0.1 \leq \mu \leq 2\farcs5$ yr^{-1} (La Bonte 1970), a limit based solely on Luyten's ability to discern motion between the original and retake plates of the Palomar Observatory Sky Survey (POSS) and to magnitudes $m_{pg} \leq 20$, the rough magnitude limit of the POSS blue plate (red main-sequence companions fainter than this magnitude were not visible on the blue plate).

In principle it was not essential to restrict our sample to those pairs with one dM star but we chose to do so for several reasons. First, dM stars are the most likely companions to the WDs in the Luyten sample. Moreover, dM stars are by far the most common type of star in the Galaxy, span the largest range of ages, and include a variety of population types. Second, prominent absorption features such as Hα of dM stars provide a fairly simple and accurate means of measuring the radial velocity (v_r) of the system (for a detailed discussion of this procedure see Silvestri et al. 2001). Third, the well-determined relationship between calcium-hydride (CaH) and titanium oxide (TiO) absorption features near Hα in dM spectra yields robust determinations of metallicity and population membership by using the CaH2 and TiO5 indices defined by Gizis (1997) and RSH. Fourth, though most of the dM's are faint, their spectral energy distributions peak in the red to near-infrared region. Hence, they are easily observed using a 4 m class telescope with moderate exposure times (30–40 minutes). Centering the spectrograph's grating on 6700 Å we simultaneously observed Hα, along with a myriad of TiO, CaH, and CaOH features. Thus one exposure for each dM star yielded an accurate v_r, metallicity, and spectral type (T_{eff}) for each dM, and the intrinsic radial velocity and population membership of each WD companion. In fact, for the purposes of this study, the WD companion did not need to be observed, as long as it was known to be a WD (as mentioned above, all WDs in our sample were spectroscopically identified by Oswalt et al. 1993). Finally, the large semimajor axes of wide binary systems ($\langle a \rangle \sim 10^3$ AU; Oswalt et al.

1993) suggest that mass exchange between the components is unlikely (Greenstein 1986; Wood & Oswalt 1992) and that each component evolves as a single star. There is no evidence to suggest that WDs in wide binary systems are different in any way from WDs without companions. Therefore the wide binaries in our sample are excellent for comparison with large samples of single WD stars.

A total of 116 WD + dM binaries were observed on the 3.5 m telescope at the Apache Point Observatory (APO) on nearly 30 half-nights between 2000 September 4 and 2001 October 20. We used the APO Double Imaging Spectrograph with a 1.″5 slit, which yielded a resolution of approximately 2 Å pixel^{-1}. The data were reduced using standard IRAF[2] reduction procedures. The data were bias-corrected and flat field–normalized. Each spectrum was extracted and wavelength calibrated using HeNeAr arc lamp spectra, and flux calibrated using the spectrum of one or more standard stars observed on the same night as the object spectrum.

Table 1 gives the observed data for all 116 WD + dM binaries. Columns (1)–(3) list the WD name assigned by Luyten, right ascension, and declination (coordinates are for epoch 1950). Columns (4)–(9) list the proper motion, its position angle, our measured radial velocity (v_r), the error in the radial velocity (σ_{v_r}), the V magnitude from Smith (1997), and M_V determined from the atmosphere models of Bergeron, Saumon, & Wesemael (1995), assuming $\log g = 8.0$ WD.

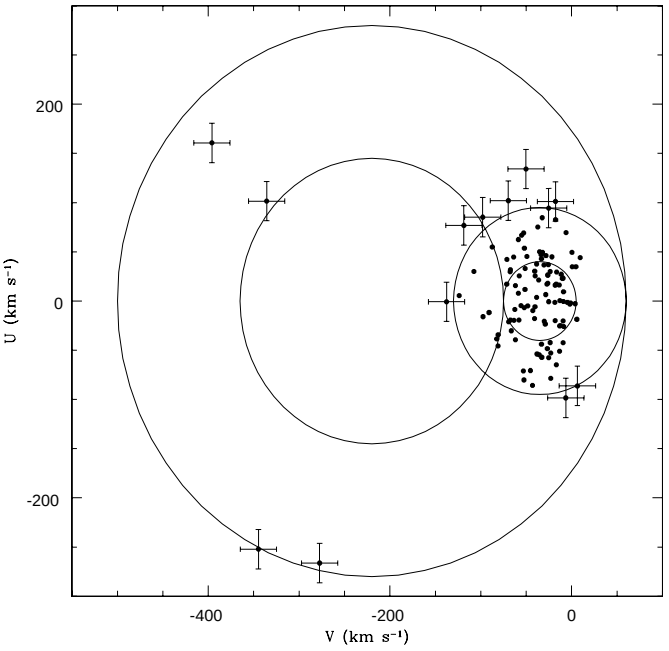

FIG. 1.—*UV*-velocity distribution of our 116 WDs with measured v_r in kilometers per second. The ellipsoids plot the 1 σ (*inner*) and 2 σ (*outer*) contours for Galactic thick-disk and stellar halo populations, respectively. The 20 km s^{-1} error bars are plotted for comparison with OHDHS for our 13 high-velocity WDs. Typical error bars for our sample are $\sim$10 km s^{-1} on average.

3. KINEMATICS

3.1. *Space Motion and Metallicity of WD + dM Binaries*

The radial velocity (v_r) of each dM was determined using the FXCOR package in IRAF. We used several well-exposed dM spectra with accurately known v_r as templates. These spanned a range of spectral types (dM1–dM6) and radial velocities (-70 km s$^{-1} \leq v_r \leq 70$ km s^{-1}). The FXCOR package determined the best-fit template spectrum to cross-correlate with a target spectrum by using a fast Fourier transform algorithm. This yielded a best-fit estimate of v_r for each dM star. Typical uncertainties were $\sigma_{v_r} = \pm$(5–10) km s^{-1}. Because the typical separation of the WD + dM pairs is $\sim 10^3$ AU (Oswalt et al. 1993) orbital velocities are negligible compared with the v_r measurement uncertainties. Hence, the v_r of a dM component gives the intrinsic v_r for each WD.

The equatorial rectangular components for each system were calculated based on its position angle, proper motion, v_r, and photometric parallax distance. The latter were determined from the *BVRI* photometry provided by Smith (1997).

The rectangular velocity components relative to the Sun for all 116 WD + dM pairs were then computed and transformed into the Galactic velocity components U, V, and W, and corrected for the peculiar solar motion $(U, V, W) = (-9, +12, +7)$ km s^{-1} (Wielen 1982). Using the measured v_r, the UVW-velocity components of the space motion for all 116 WDs were computed. The UVW-velocity components are defined as a left-handed system with U positive in the direction radially outward from the Galactic center, V positive in the direction of Galactic rotation, and W positive perpendicular to the plane of the Galaxy in the direction of the north Galactic pole. This is consistent with the orientation used by OHDHS. For comparison with the OHDHS sample our UV-velocities are displayed in Figure 1.

Unlike previous WD studies, here we can assess the full UVW space motions of our sample. In Figure 1, 13 WDs lie outside the 2 σ velocity contour centered on $(U, V) = (0, -35)$ km s^{-1} defined for disk stars (Chiba & Beers 2000). The larger set of contours, centered at $(U, V) = (0, -220)$ km s^{-1}, are 1 and 2 σ velocity ellipsoids for stars in the Galactic stellar halo as defined by Chiba & Beers (2000). Figure 2*a*–2*b* presents the UW- and WV-velocity space, respectively. Following the reasoning used by OHDHS, stars with $[U^2 + (V + 35)^2]^{1/2} > 94$ km s^{-1} were tentatively identified as halo WDs. The 13 high-velocity WDs are plotted with 20 km s^{-1} error bars in each figure as in OHDHS and RSH. They mostly arise from uncertainties in assigning distances from photometric parallaxes.

Following the discussion by RSH we plot the ratio of the CaH2 feature versus the TiO5 feature for the 116 dM's (Fig. 3). This well-defined relationship determines the metallicity, hence population membership of the dM's in our sample. Halo stars have metallicities [Fe/H] $\lesssim -1$ and exhibit weaker TiO absorption at the same CaH absorption strength (Gizis 1997). Such objects would lie in Figure 3 (*lower right*). Like Figure 4 from RSH, nearly all our dM's show near solar-type metallicity. Only LP 164-52 appears to be metal-poor, and thus it is probably a member of the stel-

[2] IRAF is written and supported by the IRAF programming group at the National Optical Astronomy Observatories (NOAO) in Tucson, Arizona. NOAO is operated by the Association of Universities for Research in Astronomy, Inc., under cooperative agreement with the National Science Foundation.

TABLE 1

116 White Dwarfs in Common Proper-Motion Binary Systems

Identifier (1)	R.A. (B1950) (2)	Decl. (B1950) (3)	μ (arcsec yr^{-1}) (4)	Θ (deg) (5)	v_r (km s^{-1}) (6)	σ_{v_r} (km s^{-1}) (7)	V[b] (8)	M_V (9)
LP 349-13	00.3683	27.4000	0.12	90	48.5	3.5	16.86	12.2
G158−78	00.3911	−10.8917	0.27	160	52.1	6.3	16.23	12.3
G171−B10A	00.3981	38.8733	0.20	132	19.4	2.9	15.97	14.1
G218−8	00.6417	55.5589	0.32	103	20.5	8.4	14.2	12.6
LP 1-170	01.0167	86.6667	0.13	73	23.6	5.0	15.2	9.3
LP 587-53	01.3450	−02.4133	0.22	79	9.8	8.9	17.48	14.1
G34−49	01.7086	23.0467	0.32	112	32.8	7.4	13.1	9.7
LP 352-30	01.7517	21.5333	0.20	80	15.3	7.2	18.32	12.6
G244−36	01.8033	64.1900	0.29	129	14.3	7.5	13.96	12.8
G71−B5B	01.8419	08.9450	0.10	154	31.3	6.6	17.22	13.2
LP 245-18	02.2892	37.5633	0.35	102	5.8	8.6	13.8	11.1
LP 590-143	02.4311	00.4083	0.11	155	13.9	8.3	18.08	14.1
LP 355-10	02.9617	24.7000	0.18	124	−26.4	8.0	16.8	8.8
LP 472-39	03.2883	11.4000	0.18	192	9.6	6.6	19.05	9.9
LP 31-139	03.4083	73.8500	0.43	141	0.0	7.6	17.50	15.7
LP 356-88	03.4167	26.3500	0.18	120	−10.8	6.7	17.66	14.5
LP 773-11	03.5300	−16.0833	0.32	80	13.9	9.2	18.52	16.5
LP 31-277	03.9100	70.7833	0.17	74	5.0	7.3	18.37	16.5
LP 415-2	04.2867	19.7833	0.17	216	−23.0	6.9	17.88	13.7
LP 775-53	04.3239	−16.1183	0.35	112	37.8	5.9	17.42	14.8
G175−34B	04.4489	58.8667	2.37	146	2.0	9.8	12.39	13.4
HZ 9A	04.4900	17.6333	0.12	110	−10.4	9.7	18.0	11.2
LP 358-52A	04.5483	26.9333	0.11	108	23.4	6.0	18.75	17.1
G86−B1B	05.3072	33.3200	0.18	113	52.4	9.2	15.98	13.5
LP 600-42	06.4689	−02.0617	0.25	214	−14.9	7.8	15.36	15.1
LP 205-27	06.6972	43.8100	0.12	176	−11.7	8.3	15.53	10.6
G87−29	07.1144	37.7567	0.44	222	−4.5	10.2	15.60	13.4
LP 422-6	07.1550	19.4000	0.10	147	−4.2	7.9	17.19	11.1
LP 5-73	07.4333	82.7333	0.18	76	14.4	7.8	15.1	9.9
LP 207-7	07.4350	39.2833	0.12	186	44.3	9.5	15.81	10.5
G107−70	07.4506	48.3183	1.34	191	−0.9	10.5	14.65	15.0
LP 783-3	07.6342	−17.2900	1.26	117	−10.0	13.4	13.05	12.9
LP 366-3	07.6936	24.8400	0.10	260	−13.1	6.6	16.52	11.5
LP 208-32	08.0717	44.6667	0.10	200	3.8	8.6	17.77	15.1
LP 664-15	08.1083	−04.3833	0.12	182	18.7	6.8	18.26	14.9
LP 163-121	08.1233	48.4167	0.14	79	17.9	9.5	18.10	13.8
G111−71	08.2797	38.7383	0.38	212	19.8	6.5	13.1	10.1
LP 164-52[a]	08.7133	49.6167	0.31	159	23.9	12.2	18.31	13.4
LP 844-26	08.8617	−24.6000	0.64	78	−0.0	15.8	18.07	14.1
LP 60-360	08.8733	63.0500	0.11	110	22.1	18.8	16.9	14.8
LP 90-70	08.9278	60.4717	0.53	216	−0.7	8.0	16.34	12.5
LP 845-8	08.9783	−22.0333	0.19	319	26.8	6.5	18.37	15.9
LP 60-178	08.9917	68.2833	0.16	215	12.8	5.4	15.1	9.0
LP 313-12	09.0750	27.8167	0.13	160	11.1	10.8	17.97	13.5
LP 313-16	09.1050	29.7000	0.14	237	23.9	7.0	15.74	11.5
LP 60-236	09.1900	65.1500	0.14	241	17.6	7.6	13.6	9.4
LP 487-25	09.2667	11.1833	0.35	235	8.6	9.9	18.38	14.9
G117−B15A	09.3536	35.4967	0.14	264	2.2	9.4	15.45	11.8
G161−36	09.4475	−03.9500	0.27	274	13.7	9.9	14.76	11.3
LP 488-19	09.6283	09.3500	0.26	255	10.1	10.1	18.09	15.9
LP 370-41	09.6833	22.5667	0.12	201	−21.7	7.9	17.14	11.6
G117−B11B	09.7231	33.0883	0.14	133	10.9	9.3	17.12	14.0
LP 62-35	10.0767	66.5667	0.21	224	22.6	11.1	12.29	8.3
LP 791-55	10.7250	−18.8333	1.98	250	40.2	6.5	15.49	15.3
LP 317-26	10.9067	30.5000	0.16	270	35.9	7.8	17.89	13.7
LP 214-38	11.0867	41.2667	0.21	275	34.6	9.2	16.25	14.0
LP 672-1	11.0917	−04.8833	0.44	184	24.0	7.1	13.10	11.0
LP 792-5	11.1917	−18.7833	0.25	300	24.8	9.4	18.33	15.0
LP 552-49	11.3483	07.3000	0.20	110	39.5	8.6	17.49	15.8
G148−7	11.7225	32.1033	0.28	203	23.2	10.6	13.73	11.1
LP 375-51	11.7961	25.5883	0.30	252	14.7	10.9	15.66	12.0
LP 129-587	11.8133	54.4667	0.25	264	6.0	6.0	16.65	12.3
LP 554-65	12.2383	03.2333	0.70	293	31.1	10.4	13.3	12.0

TABLE 1—*Continued*

Identifier (1)	R.A. (B1950) (2)	Decl. (B1950) (3)	μ (arcsec yr^{-1}) (4)	Θ (deg) (5)	v_r (km s^{-1}) (6)	σ_{v_r} (km s^{-1}) (7)	V[b] (8)	M_V (9)
LP 320-643.....	12.2517	32.3667	0.26	234	15.0	7.3	16.99	14.2
LP 435-58.....	12.3400	19.1000	0.19	268	14.2	7.1	17.26	12.4
LP 795-13.....	12.3800	−16.8333	0.12	211	45.9	8.8	18.19	12.6
G61−17	12.7456	14.9733	0.43	298	20.2	5.1	15.82	12.2
HZ 43A.....	13.2333	29.3667	0.16	240	44.4	14.4	18.6	9.9
G14−58	13.4581	−08.3133	1.24	247	35.6	4.7	12.33	11.1
LP 798-13.....	13.5717	−16.0667	0.12	246	54.1	2.6	15.33	11.5
LP 738-43.....	13.5800	−11.8000	0.19	199	35.0	9.3	18.10	13.8
LP 498-26.....	13.6125	12.3967	0.19	134	50.2	9.1	14.72	10.6
LP 856-53.....	13.8083	−27.3167	0.24	199	49.9	4.2	15.20	13.0
LP 133-374.....	14.0400	50.6000	0.20	308	13.9	9.8	18.42	15.7
LP 799-73.....	14.1600	−18.4833	0.19	133	29.7	6.0	17.12	14.2
G200−39	14.4330	54.0167	0.39	294	33.7	7.8	15.06	11.3
LP 135-154.....	15.1761	56.6033	0.38	217	13.5	9.7	16.33	12.4
LP 223-13.....	15.4250	43.3917	0.14	186	32.4	5.0	16.47	11.9
LP 176-60.....	15.5533	46.9833	0.51	296	11.4	10.5	18.23	15.7
LP 916-27.....	15.7003	−27.5000	0.24	235	−8.1	6.7	15.38	11.9
LP 101-16.....	16.5583	57.2500	1.62	319	3.4	12.5	15.05	13.4
LP 505-44.....	16.5833	11.2667	0.17	159	1.2	2.1	14.7	10.2
LP 686-32.....	16.9367	−6.1833	0.35	111	−24.8	9.0	17.21	14.6
LP 387-36.....	17.0650	26.1667	0.28	185	3.9	6.6	17.17	14.7
W672A	17.2681	2.0033	0.50	232	−19.0	1.8	14.36	11.7
G154−B5B	17.7178	−13.2883	0.09	25	−2.1	3.8	11.9	8.9
LP 230-20.....	18.9917	42.9333	0.26	201	−10.2	11.3	17.71	14.6
G142−B2A	19.1889	13.5217	0.10	180	2.6	1.8	12.7	10.4
L852-37.....	19.5483	−13.6000	0.14	189	54.0	4.8	16.05	10.9
G24−9	20.1922	06.5417	0.70	206	29.9	5.5	15.78	13.9
LP 575-16.....	20.4600	07.3333	0.26	135	27.9	3.6	16.14	12.8
LP 696-4	20.7450	−04.3000	0.20	199	25.9	5.0	17.14	12.6
VB 11	20.9017	−04.9500	0.82	105	−8.0	11.0	16.71	15.8
G212−B1A	21.1331	42.7356	0.20	98	2.2	6.9	15.62	11.7
LP 698-4	21.5133	−06.4000	0.33	205	−2.4	3.8	18.52	11.6
LP 187-7	21.5575	46.3383	0.46	200	3.0	8.5	17.97	16.7
LP 398-18.....	21.6417	21.4500	0.12	195	−0.8	7.0	17.90	12.2
LP 699-30.....	22.0300	−03.7667	0.24	90	1.4	9.0	18.26	18.0
LP 343-34.....	22.2167	31.7167	0.13	188	5.3	8.1	17.00	14.1
LP 188-2	22.4031	48.3617	0.59	41	−10.8	8.0	13.0	12.8
LP 400-22.....	22.5683	22.2800	0.20	74	7.3	9.1	17.22	11.7
LP 761-114.....	22.8222	−10.5333	0.19	157	20.5	1.6	13.5	10.1
LP 2-697	22.8867	81.2333	0.23	63	34.1	10.0	11.8	9.4
LP 581-35.....	22.8900	05.5000	0.45	127	51.6	1.6	16.19	14.9
LP 345-27.....	22.9383	31.3167	0.15	70	26.5	6.1	13.96	10.1
LP 933-65.....	23.1594	−27.6267	0.21	98	3.6	7.1	17.08	13.2
LP 522-34.....	23.3000	12.7000	0.18	72	11.5	8.9	16.27	11.0
LP 762-54.....	23.3089	−13.7333	0.20	150	−1.2	10.2	117.00	13.7
LP 582-43.....	23.3250	09.5000	0.19	225	9.8	8.4	16.24	12.2
LP 463-26.....	23.6067	20.7500	0.33	58	32.5	7.3	18.08	15.6
LP 191-8	23.6892	47.1500	0.31	94	14.7	4.1	18.22	14.2
LP 347-4	23.6900	32.2700	0.24	256	15.7	3.3	11.7	11.2
G273−B15B	23.6958	−16.4583	0.14	210	25.5	2.2	15.97	12.3
LP 935-15.....	23.7433	−26.6650	0.36	255	49.6	5.6	16.59	13.5
LP 524-34.....	23.9033	05.3833	0.21	69	31.6	8.3	18.31	13.8
LP 347-19.....	23.9817	27.0500	0.11	106	17.9	8.8	17.34	12.5

NOTE.—Units of right ascension are hours, and units of declination are degrees.

[a] Stellar halo white dwarf candidate.

[b] All single-precision V and corresponding M_V are the M star companion magnitudes. Used for distance when WD magnitudes were unavailable.

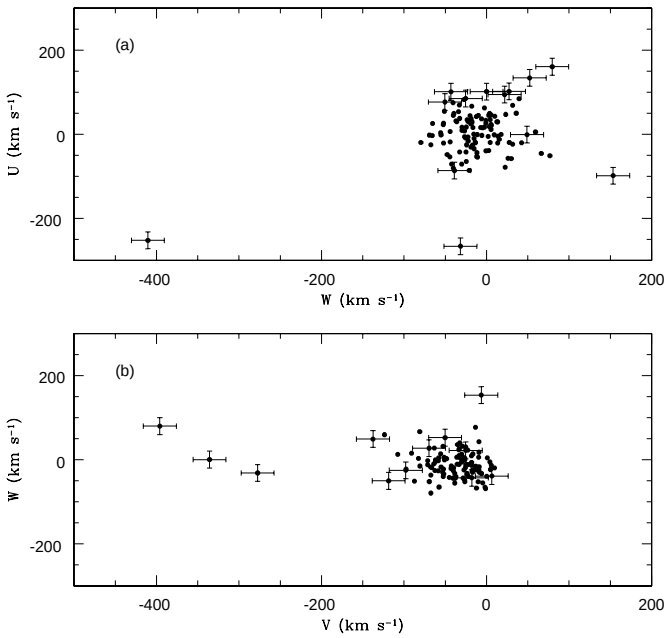

FIG. 2.—(*a*) *UW*-velocity space and (*b*) *WV*-velocity space for our WDs. The 20 km s^{-1} error bars are plotted for 13 high-velocity WDs. Error bars for the rest of the sample have been omitted for clarity.

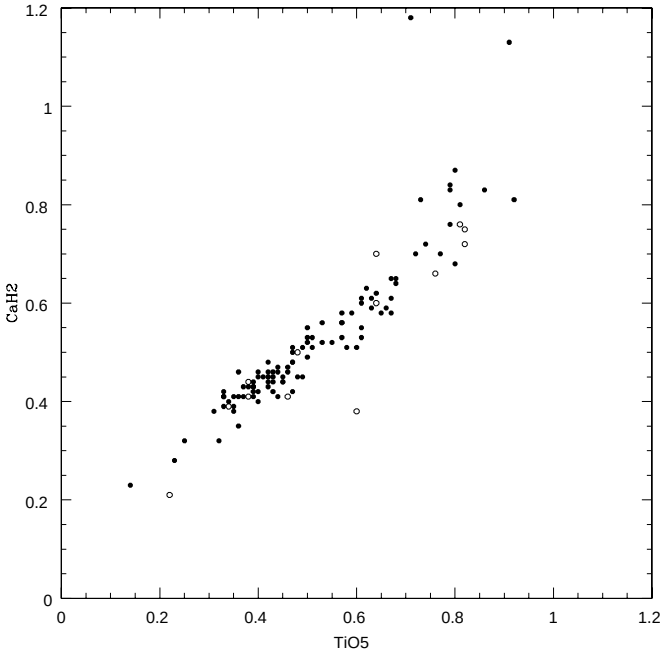

FIG. 3.—TiO5-CaH2 diagram for all 116 dM companions to the WDs plotted in Fig. 3, showing the locations of the 13 high-velocity WDs (*open circles*). The dM's (including 12 of the 13 high-velocity WDs) in our sample have near-solar abundance with the exception of the point at (0.6, 0.38), LP 164-52, which appears to be a metal-poor intermediate halo subdwarf as defined by Gizis (1997). Two stars at upper right are K stars.

lar halo population. We conclude that 115 of 116 WD + dM pairs in our sample are relatively metal-rich members of the disk.

3.2. *Comparison Assuming* $v_r = 0$ km s^{-1} *and* $W = 0$ km s^{-1}

To compare our results with those of OHDHS we applied the same assumptions they used to our analysis. There is disagreement in the literature over how best to characterize the space motion of a star when its v_r cannot be determined. In the case of single WDs, the v_r cannot be distinguished from its gravitational redshift. In the absence of a nondegenerate companion, previous studies have set $v_r = 0$ km s^{-1}. However, OHDHS argued that because their survey was confined to the south Galactic cap, the observed transverse motions were most sensitive to the *U*- and *V*-velocities. Consequently, they chose to assume $W = 0$ km s^{-1} for their WDs. Using the v_t of the 99 WDs in their sample and setting $W = 0$ km s^{-1}, OHDHS determined the v_r for each WD and then computed U and V (B. Oppenheimer 2001, private communication).

RSH found that the number of high-velocity WDs in the OHDHS sample decreased when the *U*- and *V*-velocities were computed using the more traditional assumption of $v_r = 0$ km s^{-1}. However, B. Oppenheimer (2001, private communication) has argued that the choice of assuming $W = 0$ km s^{-1} or $v_r = 0$ km s^{-1} was not important because, although some of the high-velocity stars do move in and out of the boundary outlined by the 2 σ contour, the *total number* of high-velocity WDs stays the same under either assumption. Therefore, either assumption may be valid for the OHDHS sample.

In Figure 4 we demonstrate the effect on the location of the stars in the *UV*-velocity diagram imposed when we assume $v_r = 0$ km s^{-1} versus $v_r \neq 0$ km s^{-1}. The filled circles represent the *UV*-velocities for the 116 WDs in our sample computed using their measured v_r and full space motions. The open circles represent the *UV*-velocities of our WDs computed assuming $v_r = 0$ km s^{-1}. For most of the 116 WDs the movement is minimal, and the number of high-velocity WDs (13) remains constant. For our sample, assuming $v_r = 0$ km s^{-1} when it cannot be measured does not appreciably change the fraction of high-velocity WDs detected.

Using the $W = 0$ km s^{-1} assumption we computed the *UV*-velocities for our sample. The difference in the resultant *UV*-velocities is obvious from Figure 5. Assuming $W = 0$ km s^{-1} for the stars in our sample gives the impression that many are not bound to the Galaxy. It also places nearly 3 times the number of WDs outside the 2 σ disk velocity contour. Clearly, assuming $W = 0$ km s^{-1} is not equivalent to assuming $v_r = 0$ km s^{-1} for our sample.

Consider the sky regions from which the samples discussed above were drawn. Our WDs are scattered fairly uniformly north of $-33°$, covering ~65% of the visible sky. In contrast, the OHDHS sample is constrained to the south Galactic cap in ~10% of the sky. Our sample is therefore more sensitive to motion in the *W*-direction than the OHDHS sample is, and the error from assuming $W = 0$ km s^{-1} is more pronounced. To demonstrate this, consider Figure 6*a*–6*b*, which gives a histogram of the *W*-velocity component under the $v_r = 0$ km s^{-1} assumption for both OHDHS and our samples. The OHDHS histogram (*a*) suggests $\langle W \rangle = -6.4 \pm 3.8$ km s^{-1} (σ_m), where "m" indicates "mean," while our sample (*b*) gives $\langle W \rangle = -16.2 \pm 4.4$ km s^{-1}. If we exclude the one obvious outlier at $W \sim 400$ km s^{-1} in our sample, the result becomes $\langle W \rangle = -12.9 \pm 2.9$ km s^{-1}. Thus the kinematics derived

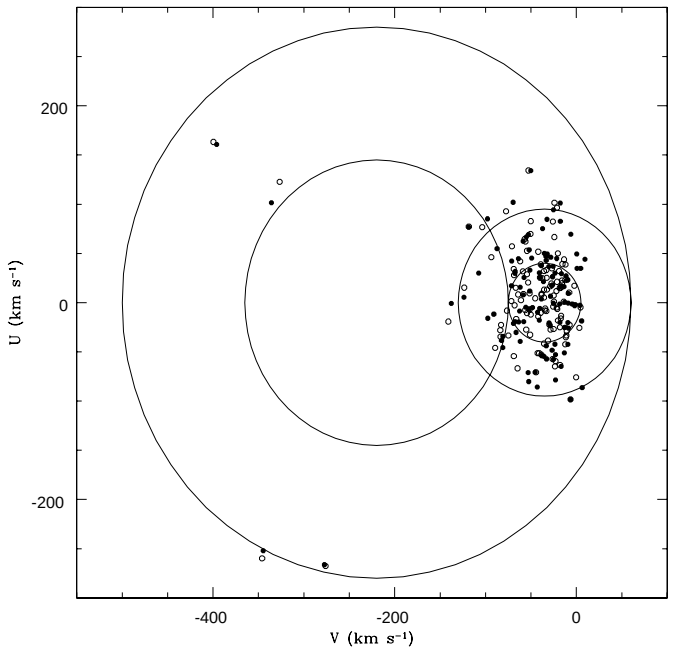

FIG. 4.—*UV*-velocity distribution of 116 WDs in kilometers per second, showing the *UV*-velocities determined for all 116 WDs by using measured v_r values (*filled circles*; see Fig. 1) and *UV*-velocities for all 116 WDs, determined on the assumption that all $v_r = 0$ km s^{-1} (*open circles*). Error bars have been omitted for clarity. Clearly, the assumption of $v_r = 0$ km s^{-1} makes very little difference in the resulting space motion components for our WDs.

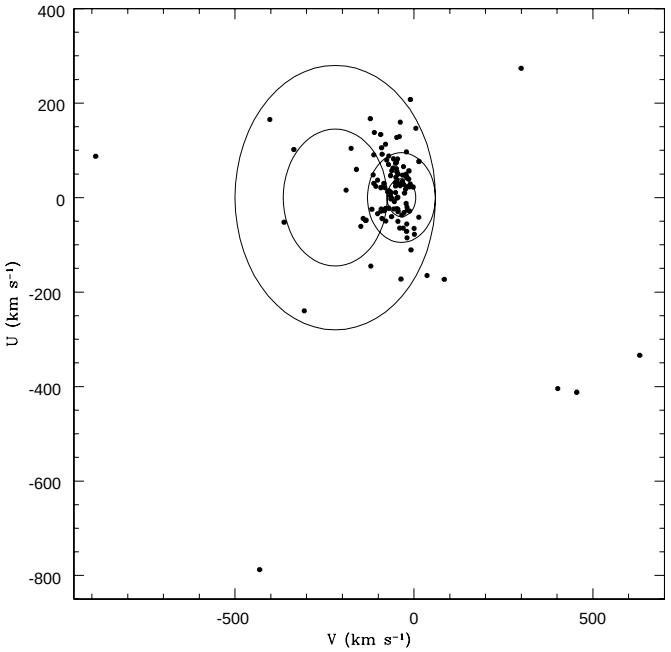

FIG. 5.—*UV*-velocity distribution of our 116 WDs in kilometers per second, determined with the assumption that $W = 0$ km s^{-1}. This assumption more than triples the number of high-velocity WDs in comparison with the number determined using either the measured v_r or the $v_r = 0$ km s^{-1} (Fig. 4) assumptions.

assuming $W = 0$ km s^{-1} rather than $v_r = 0$ km s^{-1} will exaggerate the number of high-velocity objects in our sample. The effect is lessened in the OHDHS sample because it is restricted to the polar cap.

We also considered biases introduced by the μ limits of the samples. The μ range of our sample is $0.1 \leq \mu \leq 2\farcs5$ yr^{-1}. The OHDHS sample excluded all stars with $\mu \leq 0\farcs33$ yr^{-1} and excluded all stars with $\mu > 3''$ yr^{-1}. This leads to a paucity of stars in the OHDHS sample with low space motions and no stars in either sample with extremely high space motions. Of the 33 stars in our sample that lie outside the 2 σ contour in Figure 5, 26 have $\mu < 0\farcs33$ yr^{-1}, and of the nine stars most greatly affected by the $W = 0$ km s^{-1} assumption, seven have $\mu < 0\farcs33$ yr^{-1} (see Reylé et al. 2001; Flynn, Holopainen, & Holmberg 2002, for a detailed analysis of the OHDHS μ limits).

It may seem counterintuitive that the dispersion in W decreases when low-μ objects are excluded. However, an object with low μ may still have a large v_r, which in some cases translates to a large W-velocity. Removal of such objects with large v_r then reduces the scatter in W by removing objects with large W-velocities. Also, inclusion of many low-μ objects tightens the dispersion about the mean in U, V, and W. This happens to be the case with several of our WDs. OHDHS excluded stars with these proper motions ($\mu \leq 0\farcs33$ yr^{-1}) from their sample. This may also help explain why they did not see a significant difference in resultant *UV*-velocities between the $v_r = 0$ km s^{-1} and the $W = 0$ km s^{-1} assumptions. *It also suggests that the OHDHS sample missed a significant number of what they would consider high-velocity WDs with halo-like kinematics*. Because of the omission of both low- and high-μ objects we understand that neither OHDHS nor our sample fully represents the underlying velocity dispersion of the thick disk. However, our results are consistent with what is known about the stellar disk and halo populations of the Galaxy.

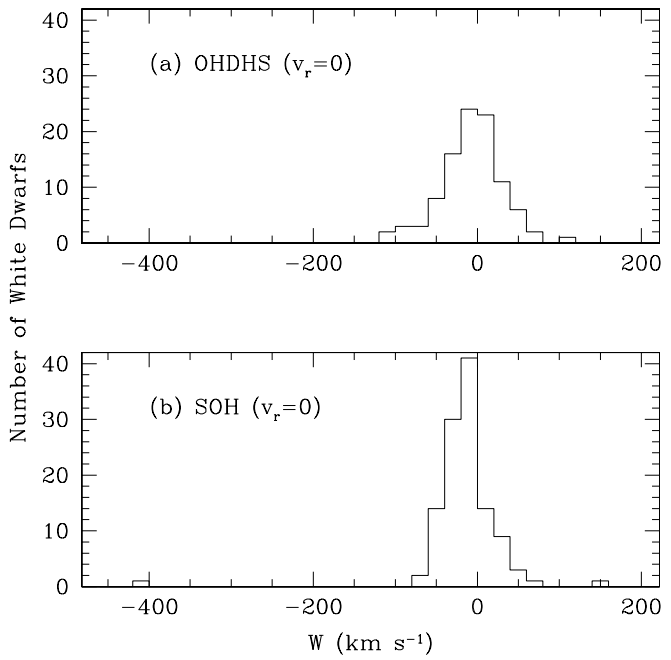

FIG. 6.—*W*-velocity histograms in kilometers per second for (*a*) the OHDHS sample, with $\langle W \rangle = -6.36 \pm 3.81$ km s^{-1} and (*b*) our sample, with $\langle W \rangle = -16.23 \pm 4.40$ km s^{-1} (omitting the WD at $\sim$400 km s^{-1}, $\langle W \rangle = -12.85 \pm 2.85$ km s^{-1}). Bin sizes are are on the order of the errors (20 km s^{-1}).

TABLE 2
U-, *V*-, AND *W*-VELOCITY DISPERSIONS

Objects	σ_U (km^{-1})	σ_V (km^{-1})	σ_W (km^{-1})	Ref.	Notes
WD + dM all.....	57	61	47	1	Entire sample of 116 stars
WD + dM 3 σ.....	46	27	26	1	Sample with 3 σ stars removed[a]
WD + dM > 0.33.....	54	29	47	1	Sample with $\mu > 0\farcs33$ yr^{-1} limit
WD > 0.33.....	92	75	38	2	Entire sample of 99 stars
WD 3 σ > 0.33	88	58	36	2	Sample with 3 σ stars removed
Stellar halo.....	141	106	94	3	$Z < 1$ kpc scale height
Thick disk	46	50	35	3	$Z < 1$ kpc scale height

[a] Refer to § 4 for a discussion of the 3 σ cut.

REFERENCES.—(1) Data from this study; (2) Oppenheimer et al. 2001a; (3) Chiba & Beers 2000.

4. COMPARISONS OF KINEMATICS WITH THAT OF KNOWN GALACTIC POPULATIONS

We next compute the velocity dispersions of our sample and the OHDHS sample and compare these with the velocity dispersions for the thick disk and halo populations given in Chiba & Beers (2000), as listed in Table 2. Figure 7 compares the *U*-, *V*-, and *W*-velocity dispersions for several different cuts of our sample to that of the thick disk (*line of unit slope*). Our full sample of 116 stars (*filled circles*) tracks very closely that expected for the thick disk. That each dispersion is ~10 km s^{-1} broader than that given by Chiba & Beers (2000) suggests that there may be a few halo objects in it (our metallicity analysis implies only one). Applying a 3 σ cut to our data (*open circles*) eliminates several (1–3) objects in the *U*, *V*, or *W* samples and moves our dispersion values closer to or below that expected for the thick disk. However, note that limiting our sample to only those 28 stars with $\mu \geq 0\farcs33$ yr^{-1} as in OHDHS also decreases the dispersions in approximately the same way.

A similar comparison of the OHDHS sample (*filled and open triangles*) in Figure 7 indicates that it has a significantly higher dispersion in *U* and *V* than ours and also higher than that expected for a pure disk sample, although the velocity dispersion in *W* agrees well. Are these higher dispersions indicative of halo membership? Figure 8 suggests not. Compared with the velocity dispersions expected for the stellar halo given by Chiba & Beers (2000; *line*), both our sample (*filled and open circles and squares*) and that of OHDHS (*filled and open triangles*) are well below those expected. The

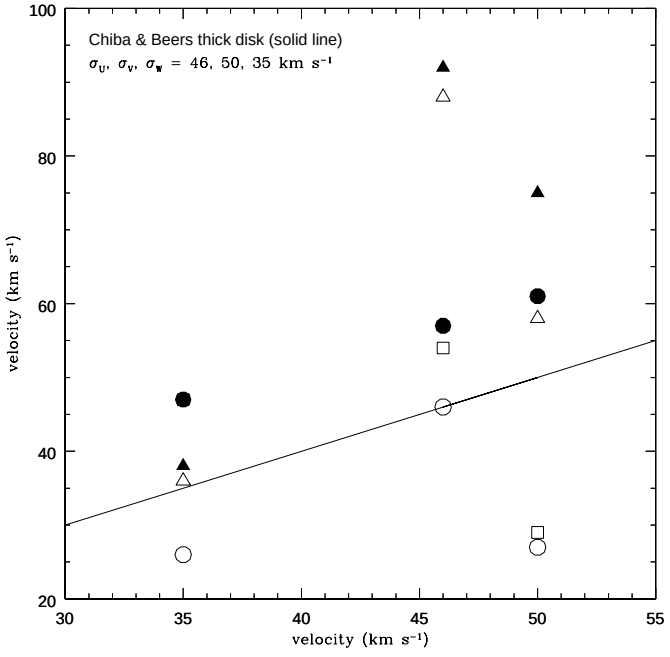

FIG. 7.—Comparison of the *U*-, *V*-, and *W*-dispersions (σ_U, σ_V, σ_W) for our sample and that of OHDHS with respect to the thick-disk velocities given by Chiba & Beers (2000; *line*), showing the 116 WDs in our sample (*filled circles*), our sample with 3 σ outliers removed (*open circles*), the $\mu > 0\farcs33$ yr^{-1} cut to our sample (*squares*), the OHDHS full sample (*filled triangles*), and the OHDHS sample with 3 σ outliers removed (*open triangles*). Note that the square lies on top of the filled circle for σ_W. Regardless of the velocity cut to either sample the dispersions in each vector cluster about the average values for the thick disk.

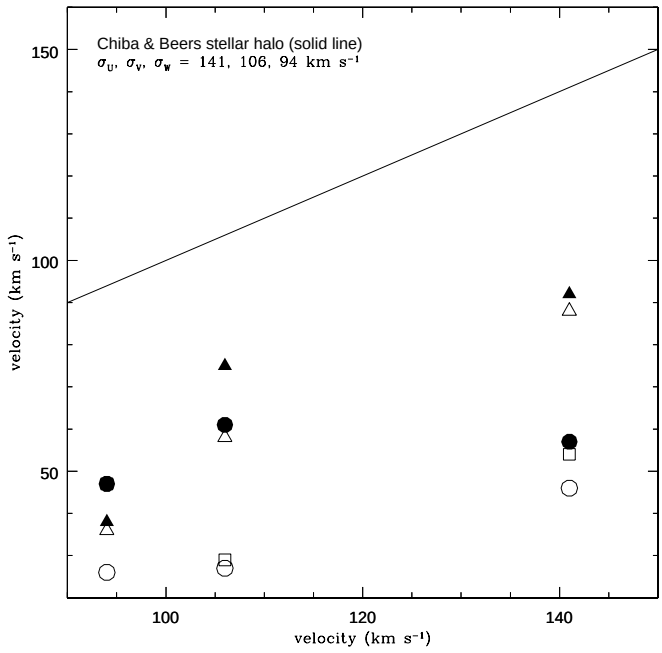

FIG. 8.—Comparison of the *U*-, *V*-, and *W*-dispersions (σ_U, σ_V, σ_W) for our sample and that of OHDHS with respect to the stellar halo velocities given by Chiba & Beers (2000; *line*), showing 116 WDs in our sample (*filled circles*), our sample with 3 σ outliers removed (*open circles*), the $\mu > 0\farcs33$ yr^{-1} cut to our sample (*squares*), the OHDHS full sample (*filled triangles*), and the OHDHS sample with 3 σ outliers removed (*open triangles*). Note that the square lies on top of the filled circle for σ_W. Obviously neither sample's dispersions are indicative of the stellar halo.

most plausible conjecture is that both samples are composed largely of disk objects, with but a small admixture of true stellar halo objects of high velocity. We thus corroborate the main hypothesis advanced by RSH, Koopmans & Blandford (2002), Reylé et al. (2001), and Flynn et al. (2002).

One final comparison can be made, which also supports our contention that the OHDHS sample is overwhelmingly from the thick disk. OHDHS note that 11 of their 38 (29%) high-velocity halo WD candidates were also found by Luyten and assigned LHS or LP numbers. In our sample only 1 of 116 stars are likely to be true halo WDs, based on our metallicity study of dM companions. Using the ratio of overlap, we estimate that the OHDHS should contain at most $\sim$3 times the number of stellar halo WDs as our sample, or about 3 objects. This is an order of magnitude less than the 38 claimed by OHDHS and in line with the stellar halo WD space density expected in the solar neighborhood (Gould et al. 1998).

5. CONCLUSIONS

In the context of previous work discussed above, our analysis suggests that nearly all our sample and the overwhelming majority of the OHDHS high-velocity WDs are members of the Galactic disk. We also add one new WD (LP 164-52) to the growing list of stellar halo WD candidates. Our study of WD + dM systems demonstrates that partial kinematic data are not sufficient to distinguish between disk and stellar halo membership even in relatively large samples of stars. The metallicities afforded by dM companions provide essential confirmation of population membership.

In our all-sky sample, assuming that one component of the space motion is zero ($W = 0$ km s^{-1} in this case) would impose large errors in the nonzero components of the space motion and yield a distorted view of the sample's overall kinematical properties. In both samples assuming the v_r changes the U-, V-, and W-velocity of an individual star, an assumption of $v_r = 0$ km s^{-1} for a large sample of stars still yields a realistic view of the overall kinematics and allows for less complicated comparison between large samples of stars.

Our sample and the OHDHS sample clearly possess stars that are part of a rotating component and have kinematics that resemble the high-velocity tail of the Galaxy's disk population. Also, the dM stars in our sample exhibit metallicities indicative of the thick-disk component of the Galaxy, just as RSH demonstrated with their large sample of dM stars. Thus, we conclude that most of the high-velocity WDs in the OHDHS study are *not* stellar halo WDs and that their space density and contribution to the dark matter halo content has been greatly overestimated. It is clear, however, that the OHDHS sample does contain a substantial number of cool blue degenerates. For that reason alone it warrants extensive investigation since it is likely to yield valuable information on the white dwarf luminosity function and age of the Galactic disk.

The authors would like to thank Ben Oppenheimer for several helpful conversations about the OHDHS sample and the staff at Apache Point Observatory for their help during our observing runs. This work was supported in part by the NASA Graduate Researchers Program Grant NGT 200415 and a Grant-in-Aid of Research from the National Academy of Sciences administered by Sigma Xi, the Scientific Research Society (N. M. S.), NSF grant AST 90-16284, and NASA grant NAGW5-9408 (T. D. O.).

REFERENCES

Alcock, C. 2000, ApJ, 542, 281
Bergeron, P. 2001, ApJ, 558, 399
Bergeron, P., Ruiz, M.-T., Leggett, S. K., Saumon, D., & Wesemael, F. 1994, ApJ, 423, 456
Bergeron, P., Saumon, D., & Wesemael, F. 1995, ApJ, 443, 764
Chiba, M., & Beers, T. C. 2000, AJ, 119, 2843
Davies, M. B., King, A., & Ritter, H. 2002, MNRAS, 333, 463
Dawson, P. C. 1986, ApJ, 311, 984
Flynn, C., Holopainen, J., & Holmberg, J. 2002, MNRAS, in press
Gibson, B. K., & Flynn, C. 2002, Science, in press
Giclas, H. L., Burnham, R., & Thomas, N. G. 1971, in Lowell Proper Motion Survey, Northern Hemisphere: The G-Numbered Stars (Flagstaff: Lowell Observatory), 1
———. 1978, Lowell Obs. Bull. 8, 89
Gizis, J. E. 1997, AJ, 113, 806
Gould, A., Flynn, C., & Bahcall, J. N. 1998, ApJ, 503, 798
Greenstein, J. L. 1986, AJ, 92, 859
Hambly, N. C., Smartt, S. J., Hodgkin, S. T., Jameson, R. F., Kemp, S. N., Rolleston, W. R. J., & Steele, I. A. 1999, MNRAS, 309, L33
Hansen, B. 1998, Nature, 394, 860
———. 2001, ApJ, 558, L39
Ibata, R., Irwin, M., Bienaymé, O., Scholz, R., & Guibert, J. 2000, ApJ, 532, L41
Knox, R. A., Hawkins, M. R. S., & Hambly, N. C. 1999, MNRAS, 306, 736
Koopmans, L. V. E., & Blandford, R. D. 2002, MNRAS, in press
La Bonte, A. E. 1970, in IAU Colloq. 7, Proper Motions, ed. W. J. Luyten (Minneapolis: Univ. Minnesota Press), 26
Luyten, W. J. 1963, in Proper-Motion Survey with the 48 Inch Telescope (Minneapolis: Univ. Minnesota Press), 1
———. 1969, in Proper-Motion Survey with the 48 Inch Telescope (Minneapolis: Univ. Minnesota Press), 1
———. 1974, in Proper-Motion Survey with the 48 Inch Telescope (Minneapolis: Univ. Minnesota Press), 1
Luyten, W. J. 1979, in Proper-Motion Survey with the 48 Inch Telescope (Minneapolis: Univ. Minnesota Press), 1
Mendez, R., & Minniti, D. 2000, ApJ, 529, 911
Oppenheimer, B., Hambly, N. C., Digby, A. P., Hodgkin, S. T., & Saumon, D. 2001a, Science, 292, 698 (OHDHS)
Oppenheimer, B., et al. E. 2001b, ApJ, 550, 448
Oswalt, T. D., Hintzen, P. M., & Luyten, W. J. 1988, ApJS, 66, 391
Oswalt, T. D., Sion, E. M., Hintzen, P. M., & Liebert, J. W. 1991, in Proc. NATO Advanced Research Workshop: 7th European Workshop on White Dwarfs, ed. G. Vauclair & E. M. Sion (Kluwer: Dordrecht), 379
Oswalt, T. D., & Smith, J. A. 1995, in Proc. of the 9th European Workshop on White Dwarfs, ed. D. Koester & K. Werner (Berlin: Springer), 24
Oswalt, T. D., Smith, J. A., Shufelt, S., Hintzen, P. M., Leggett, S. K., Liebert, J., & Sion, E. M. 1993, in Proc. of the NATO Advanced Research Workshop: 8th European Workshop, White Dwarfs: Advances in Observation and Theory, ed. M. A. Barstow (Dordrecht: Kluwer), 419
Oswalt, T. D., Smith, J. A., Wood, M. A., & Hintzen, P. 1996, Nature, 382, 692
Reid, I. N. 1996, AJ, 111, 2000
Reid, I. N., Sahu, K. C., & Hawley, S. L. 2001, ApJ, 559, 942 (RSH)
Reylé, C., Robin, A. C., & Crézé, M. 2001, A&A, 378, L53
Saumon, D., & Jacobson, S. B. 1999, ApJ, 511, L107
Silvestri, N. M., Oswalt, T. D., Wood, M. A., Smith, J. A., Reid, I. N., & Sion, E. M. 2001, AJ, 121, 503
Smith, J. A. 1997, Ph.D. thesis, Florida Inst. Technol.
Smith, J. A., & Oswalt, T. D. 1995, in Proc. of the ESO Workshop, The Bottom of the Main Sequence—and Beyond, ed. C. G. Tinney (Berlin: Springer), 113
Wielen, R. 1982, Landolt-Börnstein Tables, Astrophysics, Vol. 2C, Sec. 8.4 (Berlin: Springer), 202
Wood, M. A., & Oswalt, T. D. 1992, ApJ, 394, L53
———. 1998, ApJ, 497, 870